Letters in Applied NanoBioScience
Open-Access Journal (ISSN: 2284-6808)

Article
Volume 13, Issue 1, 2024, 44
https://doi.org/10.33263/LIANBS131.044

Removal of a Toxic Herbicide 2,4,5-trichlorophenoxyacetic Acid Using a Recycling Eco-friendly Adsorbent

El Hassane Mourid [1,*], Mohamed Lakraimi [1], Mustapha Cherkaoui [1]

[1] Interdisciplinary Laboratory for Research in Bio-resources, Environment and Materials, Department of Chemistry, Cadi Ayyad University, Marrakech, Morocco
* Correspondence: mourice-smc@gmail.com (E.H.M.);

Scopus Author ID 57193321465

Received: 1.01.20223; Accepted: 19.03.2023; Published: 11.03.2024

Abstract: In this work, we are interested in the elimination of the herbicide 2,4,5-trichlorophenoxyacetic acid (2,4,5-T) using an adsorption process onto an eco-friendly material named LDH [Zn_2-Al-CO_3] calcined at 500 °C. Indeed, dissolving calcined LDH in a pollutant solution allows the retention of herbicide in its anionic form. The choice of LDH based on Zn and Al was conditioned by their low cost, ease of synthesis, not toxic to the environment, and not generating sludge. Several parameters were considered: the retention of pollutants by LDH nanomaterial is improved for a pH range between 5 and 6, the equilibrium retention is obtained after 6 hours, and retention kinetics follows the pseudo-second-order model. The isotherms are of L-type, and they follow the Freundlich model; retention capacity reaches 75 % for a mass ratio 2,4,5-T/CLDH of 0.66, and the maximum amount retained of the dye is 590 mg/g. X-ray diffraction showed that the synthesized matrix is crystallized in a lamellar structure; the adsorption is governed by intercalation of the herbicide in its anionic form between the reconstructed LDH sheets. Infrared analysis indicated the appearance of the characteristic bands of pollutants in the matrix spectrum, thus confirming his retention. Additionally, SEM analysis exposed the lamellar character of the phase achieved before and after the intercalation of the pollutant. LDH adsorbent can be considered a better nanomaterial with a high capacity of retention, has a low cost, and is eco-friendly.

Keywords: calcined layered double hydroxide; herbicide; depollution; adsorption; recycling.

© 2024 by the authors. This article is an open-access article distributed under the terms and conditions of the Creative Commons Attribution (CC BY) license (https://creativecommons.org/licenses/by/4.0/).

1. Introduction

While the quantity of groundwater used as a vital source is currently sufficient to meet the needs of all living things, its quality has become a matter of concern as it supports the physiological activities of living cells [1]. Growing industries and advances in technology have endangered water resources around the world. About a sixth of the world's population faces the challenge of the unavailability of freshwater [2,3]. The greatest threat to the world is water contamination, the main cause of which is the discharge from industries exposed to water bodies without correct treatment of harmful constituents [2,4]. Water contamination with organic pollutants is dangerous due to their carcinogenic nature [5]. Currently, several varieties of emerging contaminants are detected in aqueous media worldwide. These include pesticides, industrial additives, pharmaceutical compounds, surfactants, hormones, personal care products, etc. [6,7]. The protection of the environment and the problem of decontaminating

contaminated water and soil require a rapid reaction from the whole world. The pollution is often of industrial origin or agricultural, that is to say, due to the lack of necessary precautions to avoid the leakage of toxic waste such as fertilizers and pesticides. Therefore, they contribute to surface water and groundwater quality degradation through their harmful and toxic side effects.

Recently, several studies have reported the presence of traces of pesticides in foods [8,9,10], as well as in groundwater and surface water [11,12]. The toxicity of these organic pollutants is linked to their stable molecular structure, which resists degradation, or to the fact that they degrade into more dangerous and carcinogenic side products [13]. Globally, several hundred pesticide formulations and thousands of active substances are used to protect crops and improve their yield [14]. The total volume of contaminated soil and sediment is approximately 700.000 m^3. The main ingredients of contaminating herbicides are 2,4-dichlorophenoxyacetic acid (2,4-D), 2,4,5-trichlorophenoxyacetic (2,4,5-T), and dioxin. These products are often toxic to humans and the environment, even at low concentrations.

About half of Morocco's population resides in rural areas, 80% of which work in the agricultural sector. In recent years, Morocco has imported an average of 1000 tonnes of pesticides annually [15]. This use poses the problem of their fate in the environment, causing the contamination of water resources, air, and soil. Therefore, it appears necessary to study the fate of these compounds in water to better measure their consequences, particularly their environmental impact. Herbicides are among the most dangerous persistent pollutants [16]; their use so far has been considered the most economical and effective method of controlling noxious weeds in agricultural environments [17,18] and non-agricultural [19,20]. Despite their advantages, they cause water pollution and other ecological problems when they leave their application sites under different climatic factors [21]. Several methods, such as degradation using advanced oxidation, especially heterogeneous photocatalysis and adsorption, have been applied for the partial or total removal of pesticides from water [22]. Several studies have focused on the retention of herbicides by adsorption on clay materials [23], graphene oxide composite [24], activated carbon [25], and agro-food waste [21]. The review of the work on the adsorption of herbicides by soil constituents shows that adequate sis of the observed phenomena remains difficult due to the complexity of the adsorbent-adsorbate system examined and the various physical, chemical, and biological interactions [26]. Estimating the effects of pesticide-related pollution on ecosystems is difficult. Its impact depends on their mode of action, persistence over time, and degradation by-products. These metabolites are sometimes more toxic and degrade slowly than the initial compound. There are two types of toxicity: acute and chronic. Harmful effects and acute toxicity develop after the absorption process, and therefore, chronic toxicity of a substance can cause adverse health effects; it is a long-term manifestation. This toxicity impacts humans and the environment [27,28], particularly through carcinogenic, immunosuppressive, mutagenic, neurotoxic, and teratogenic effects [29,30]. From this perspective, layered double hydroxides (LDH) have been the subject of numerous investigations in fields as varied as environmental pollution control, the pharmaceutical industry, the manufacture of polymers, catalysis, electrochemistry of solids (proton conduction), etc. [23,31]. The objective of this study is to examine the effectiveness of the elimination of the herbicide 2,4,5-T by adsorption on a calcined LDH based on zinc and aluminum while by studying the effect of several reaction parameters such as the contact time, the pH of the medium, the dose of the adsorbent material, as well as the influence of the initial concentration of 2,4,5-T on the yields of its elimination.

2. Materials and Methods

2,4,5-Trichlorophenoxyacetic acid is a herbicide with the molecular formula $C_8H_5Cl_3O_3$ belonging to the family of chlorophenoxyalkanoic acids (Fig. 1). It was developed at the end of the 1940s. It is obtained by reacting 2,4,5-trichlorophenol with monochloroacetic acid at a temperature between 100 and 180°C, depending on the reaction medium and the pressure used [32].

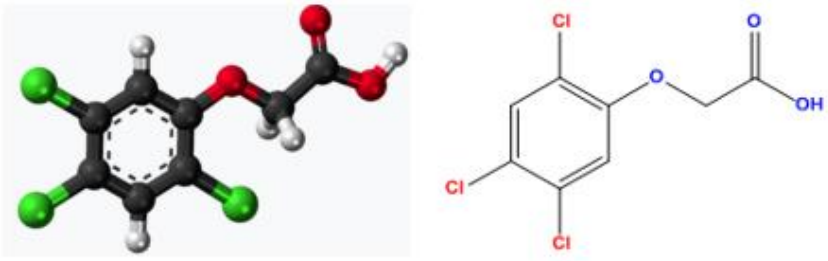

Figure 1. Chemical structure of 2,4,5-Trichlorophenoxyacetic acid.

Herbicide 2,4,5-T has been used on a large scale in agriculture worldwide to control the growth of broadleaf weeds in cereal crops, meadows, and lawns [33]. Due to its toxicity concerns, the use of 2,4,5-T has been excluded in some developed countries, but it is still widely used today in most developing countries for weed control and to improve crop yields [33]. 2,4,5-T is considered less biodegradable than its herbicidal analogue 2,4-D and exhibits resistance during degradation by microorganisms, likely due to additional chlorine on the aromatic nucleus [34]. Table 1 presents the physicochemical characteristics of 2,4,5-T herbicide.

Table 1. Physicochemical properties of 2,4,5-T.

Physical state	White powder
Molecular weight	255.49 g/mol
Solubility	275 mg/L at 20 °C
Density	1.8
pK_a	2.88 at 25 °C

2.1. Effect of pH.

pH is a factor that can alter the surface charge of the adsorbent material and the speciation distribution of adsorbate in solution. The influence of pH on the retention of 2,4,5-T was examined using 30 mg of calcined LDH in a 100 mg/L solution of 2,4,5-T stirred for 24 h under a nitrogen atmosphere. The suspensions prepared with decarbonated water are adjusted to pH values between 4 and 11 by adding a solution of HCl (0.5M) or NaOH (0.5M). The maximum amount of 2,4,5-T retained by CLDH increases for pH values between 5 and 6 (Fig. 2). The lower retention of 2,4,5-T at pH = 4 can be attributed to partial dissolution of the matrix LDH by acid hydrolysis [35].

At pH > 6, competition with CO_3^{2-} ions, known for their high affinity for LDH, could explain the progressive decrease in the retention of 2,4,5-T [23]. Therefore, all subsequent experiments were performed at a pH of 5. Within this pH range, 2,4,5-T herbicide is found in its anionic form in aqueous solution (pK_a = 2.88).

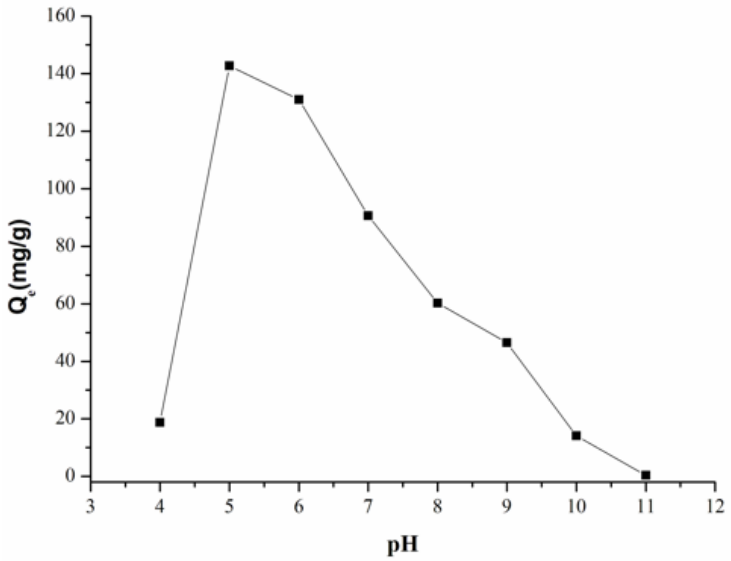

Figure 2. Quantities of 2,4,5-T retained by 30 mg of LDH as a function of the pH.

The final pH values obtained after pollutant retention as a function of the initial pH fixed in the first experiment showed the presence of a buffer zone where the pH is almost quasi-constant. The zero charge point pH (pHpzc) where the final pH versus the initial pH curve crosses the lines pH initial value equals a pH final value (Fig. 3). This point of intersection is pHpzc equal to 9. This figure showed that the surface charge of LDH is almost neutral at pHpzc. At pH < pHpzc, the LDH surface has a net positive charge, while at pH > pHpzc the surface has a net negative charge.

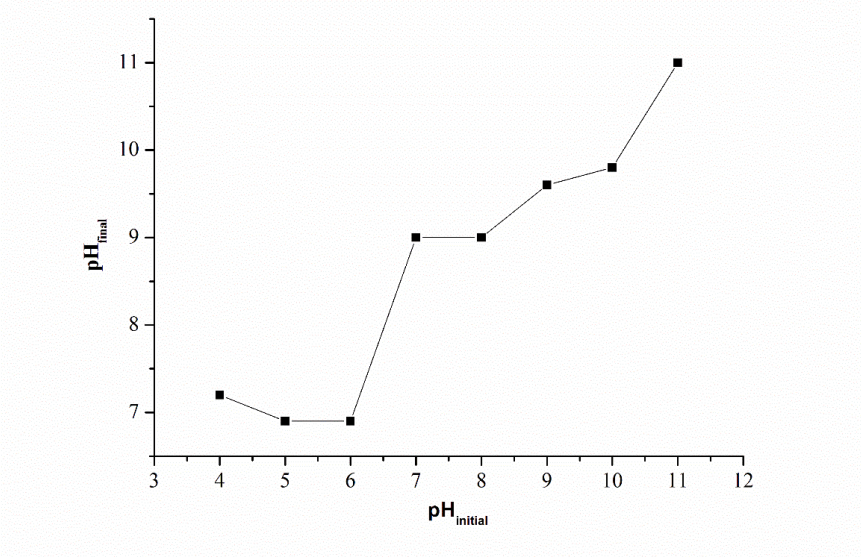

Figure 3. pHpzc in function of pH values.

2.2. Kinetic study.

The change in the quantity of 2,4,5-T herbicide retained per 30 mg of calcined LDH as a function of the contact time for different initial concentrations (20, 100, and 250 mg/L) is illustrated in Fig. 4. Retention kinetics slow as initial 2,4,5-T concentration increases. The equilibrium condition, reached in less than 3 h for a low initial concentration (20 mg/L), requires 6 h of stirring for the highest concentration, corresponding to the maximum solubility of 2,4,5 -T in an aqueous medium. Increasing the concentration of 2,4,5-T results in an increase in its retained amount per mass of LDH. These experimental data suggest that the retention process is determined, in part, by the surface interaction between the herbicide and LDH. The

relatively slower retention of 2,4,5-T as its concentration in solution increases may be due to some competition between these molecules in anionic form. Consequently, a contact time of 6 h was adopted in the remainder of this work to ensure that the state of equilibrium is reached.

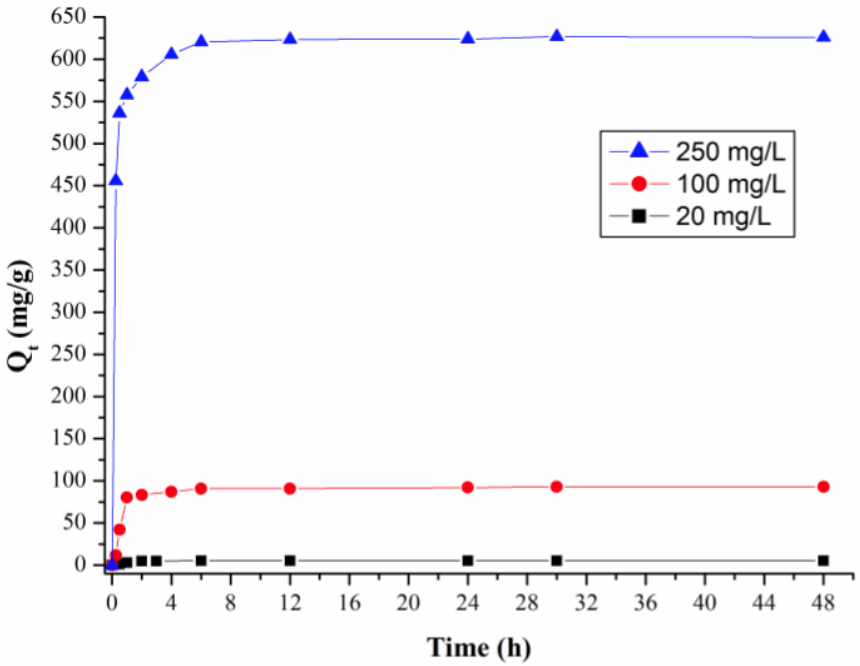

Figure 4. Adsorption kinetics of 2,4,5-T per 30 mg of LDH at concentrations of 20, 100, and 250 mg/L.

From these results, it is inferred that the retention process of 2,4,5-T is relatively rapid, suggesting that LDH has a high affinity for the herbicide 2,4,5-T. Adsorption is, therefore, probably ensured by electrostatic interactions and by hydrogen bonds [36].

2.2.1. Kinetic models.

The kinetic modeling of 2,4,5-T retention was carried out according to the two models:

The pseudo-first-order linear model according to the equation [37]:

$$\mathrm{Ln}(\mathrm{Q_e} - \mathrm{Q_t}) = \mathrm{Ln}(\mathrm{Q_e}) - k_1 \mathrm{t}$$

The pseudo-second-order linear model according to the equation [38]:

$$\frac{\mathrm{t}}{\mathrm{Q_t}} = \frac{1}{\mathrm{k_2 Q_e}^2} + \frac{1}{\mathrm{Q_e}}\mathrm{t}$$

Fig. 5 represents the kinetic models of the pseudo-first and pseudo-second order.

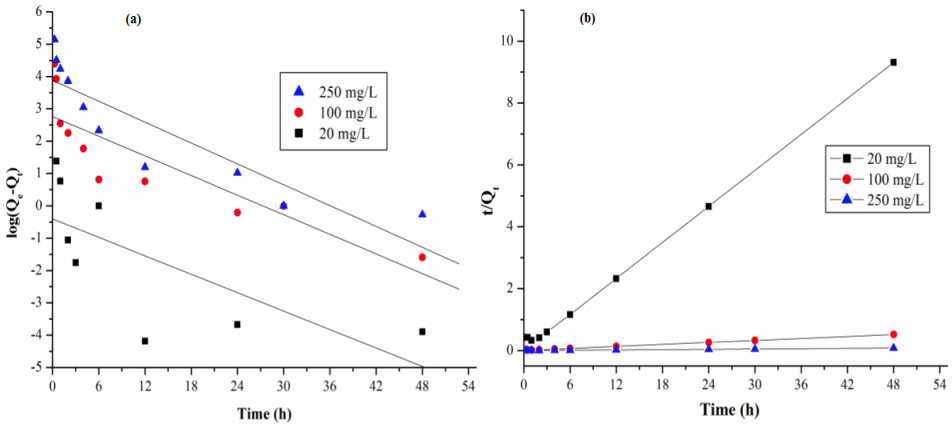

Figure 5. Pseudo-first (a) and pseudo-second-order (b) kinetic models of 2,4,5-T retention by CLDH at three initial 2,4,5-T concentrations (20, 100 and 250 mg/L).

The linear forms of these figures lead to the obtaining of the various parameters of the kinetic models and the maximum quantities of 2,4,5-T retention, which are presented in table 2 below.

Table 2. Parameters of pseudo-first and pseudo-second-order kinetic models and maximum adsorption quantities after retention of 2,4,5-T herbicide.

Pseudo-first order model					
C_0 (mg/L)	**Equation Log (Q_e-Q_t) =**	**k_1 (h^{-1})**	**$Q_{e,th}$ (mg/g)**	**$Q_{e,exp}$ (mg/g)**	**R^2**
20	-0.095·t – 0.4051	0.095	0.6	5.17	0.513
100	-0.1011·t + 2.7602	0.101	15	93.00	0.757
250	-0.1075·t + 3.8808	0.107	48	626.59	0.799
Pseudo-second order model					
C_0 (mg/L)	**Equation t/Qt =**	**k_2 (g/mg/h)**	**$Q_{e,th}$ (mg/g)**	**$Q_{e,exp}$ (mg/g)**	**R^2**
20	0.191·t + 0.0993	0.372	5.20	5.17	0.999
100	0.0106·t + 0.0058	0.019	94.00	93.00	0.999
250	0.0016·t + 0.0002	0.012	625.0	626.59	1

According to the results collected in Table 2 above, we can say that the retention kinetics of 2,4,5-T by LDH agrees with the model of the pseudo-second-order (values of R^2 close to unity). On the other hand, for the pseudo-first-order model, the values of the correlation coefficients are all different from unity. We deduce that the retention kinetics of 2,4,5-T follow the pseudo-second-order model.

2.2.2. Intra-particle diffusion.

The intraparticle diffusion model, which describes the mechanism of migration of solute anions to the solid material, was used to assess its contribution to the retention process (Fig. 6). It can be expressed by the following equation [39]:

$$Q_t = K_{id} \cdot t^{1/2} + C$$

With K_{id} being the kinetic constant and C the thickness of the double layer.

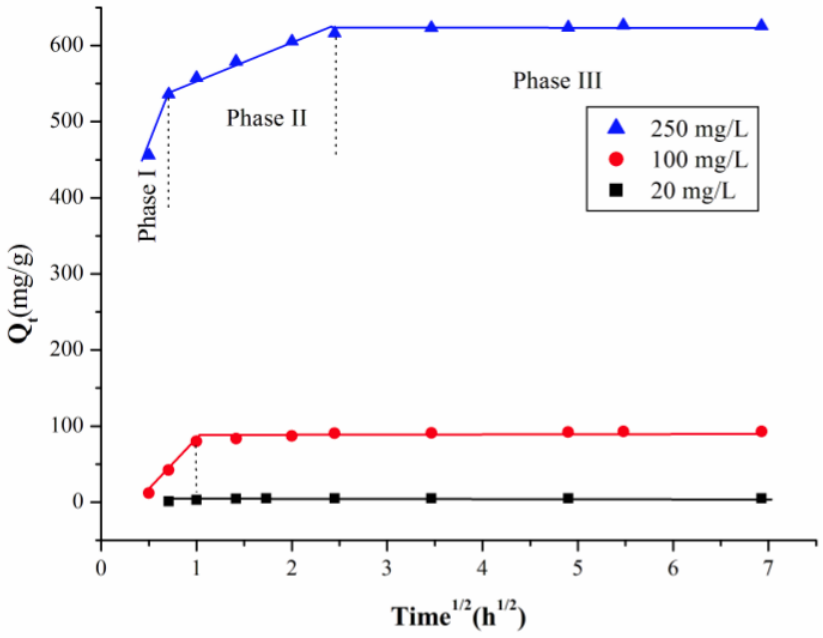

Figure 6. Linear representation of the kinetic model of intraparticle diffusion for the retention of 2,4,5-T.

The multilinearity of the graphs indicates that two or more steps occur during the interaction between 2,4,5-T and LDH, with the slower step determining the overall rate of the

retention process [40]. The linearization of the equation for the highest concentration of 2,4,5-T (250 mg/L) has three distinct phases, namely (I) adsorption on the surface of the adsorbent, diffusion and intraparticle (intercalation between reconstructed LDH sheets) (II) and the state (III) achieving steady state. The constants of this model are given in Table 3.

Table 3. Parameters of the kinetic model for intra-particle diffusion.

	phase I			phase II			phase III		
C_0 (mg/L)	K_{1p} (mg/g/$h^{1/2}$)	C (mg/g)	R^2	K_{2p} (mg/g/$h^{1/2}$)	C (mg/g)	R^2	K_{3p} (mg/g/$h^{1/2}$)	C (mg/g)	R^2
20	0.395	3.216	0.337	-	-	-	-	-	-
100	136.2	-55.46	0.998	1.894	82.23	0.715	-	-	-
250	1.175	0.119	1	45.88	509.4	0.974	1.976	613.9	0.713

2.3. Thermodynamic study.

To describe the phenomenon of adsorption in the function of temperature, this study was carried out at three temperatures, 298, 320, and 335 K, in a time interval from 30 minutes to 6 h. The pesticide concentration is maintained at 100 mg/L, and the mass of the calcined Zn_2-Al-CO_3 is 30 mg. The obtained parameters, such as enthalpy (ΔH°), entropy (ΔS°), and Gibbs free energy (ΔG°), were calculated using the following equations [41]:

$$K_c = Q_e/C_e$$

$$\text{Ln } K_c = \Delta S°/R - \Delta H°/RT$$

$$\Delta G° = -RT \text{ Ln } K_c$$

Where Q_e is the adsorption amount of adsorption (mg/g), K_c represents the equilibrium constant and the concentration of the adsorbent at equilibrium C_e (mg/L). Using the slope and the intercept of the plot of Ln K_c versus 1/T to determine the ΔH° and ΔS° values (Table 4). The negative value of ΔH° indicates that this adsorption is exothermic. The ΔG° values are negatives, confirming the spontaneous mechanism of the retention. The value of ΔH° equals -4.413 kJ/mol, which indicates that the adsorption of the pollutant 2,4,5-T by calcined Zn_2-Al-CO_3 is described by a physisorption process [42]. The value of ΔS° is negative, confirming an order at the interface between the adsorbate and the adsorbent. The decrease in the retained quantity of pesticide is also observed when the temperature increases from 298 to 335 K. This decrease can be explained by the thermal agitation, which causes the release of adsorbed pesticide molecules on sites of the reconstructed Zn_2-Al-CO_3 by the electrostatic or hydrogen bonds [41].

Table 4. Thermodynamic parameters obtained at different temperatures.

T(K)	LnK_c	Q_e(mg/g)	ΔG°(kJ/mol)	ΔH°(kJ/mol)	ΔS°(J/mol/K)
298	0.220	92.725	-0.545	-4.413	-13.079
320	0.054	80.185	-0.143		
335	0.031	67.546	-0.086		

2.4. Adsorption isotherms.

The adsorption isotherms for two different masses of CLDH (30 and 50 mg) are given in Fig. 7.

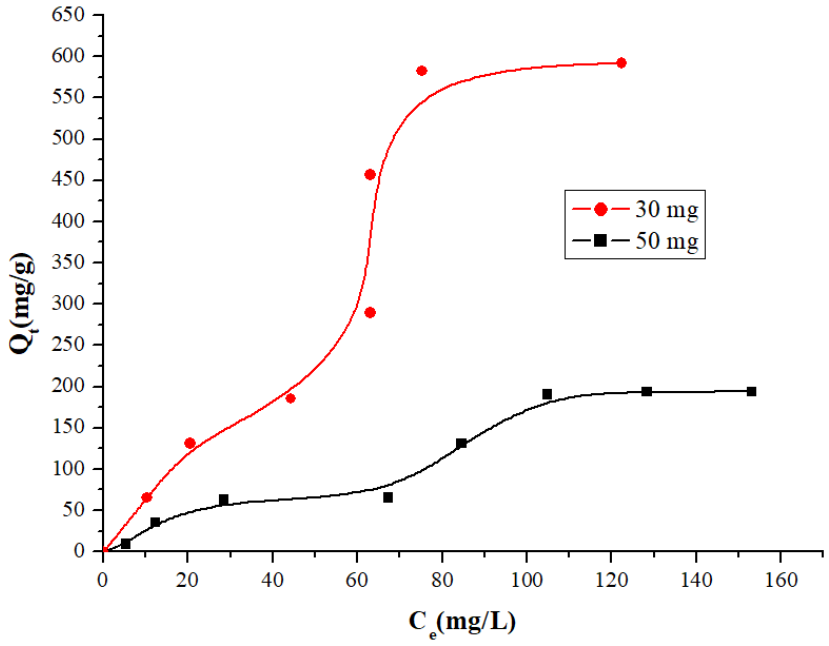

Figure 7. Quantities of 2,4,5-T retained by two different masses of CLDH as a function of the equilibrium concentration.

The shape of the two isotherms is L-type, according to the classification of Giles et al. [43], suggesting that the retention of 2,4,5-T occurs at specific adsorbent sites. Adsorption data are presented (Fig. 8) based on the linear form of two models:

Langmuir's model [44], according to the equation:

$$\frac{C_e}{Q} = \frac{1}{KQ_m} + \frac{C_e}{Q_m}$$

The linear model of Freundlich [45] according to the equation:

$$Ln(Q) = Ln(K_f) + \frac{1}{n}Ln(C_e)$$

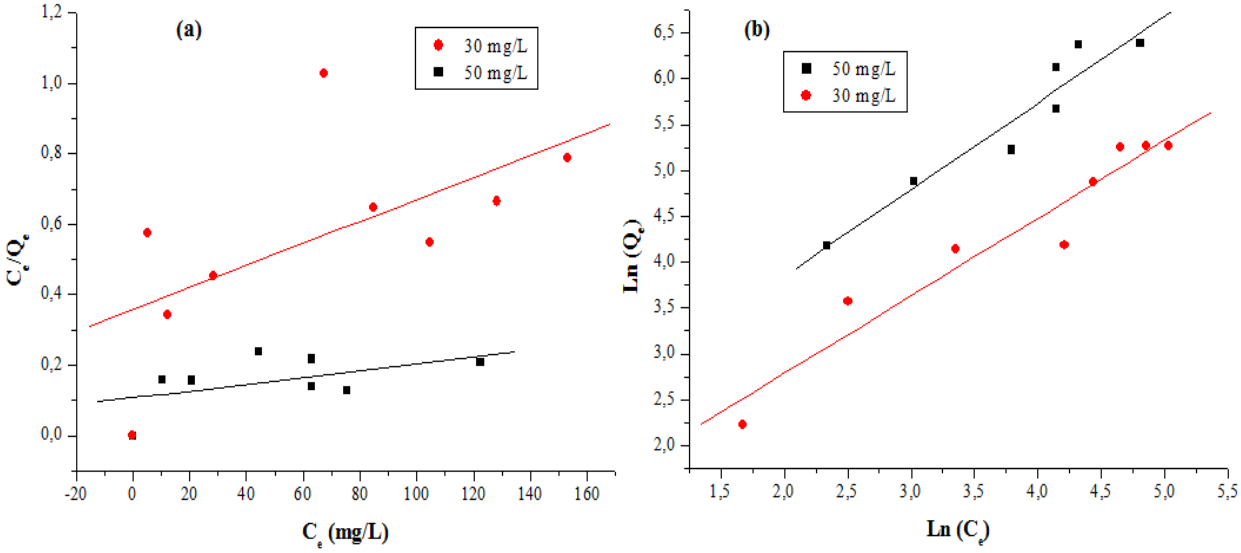

Figure 8. Linear representations of Langmuir (a) and Freundlich (b) models of 2,4,5-T adsorption on LDH adsorbent.

The values of the parameters of the Langmuir and Freundlich models are given in Table 5.

Table 5. Parameter values of the Langmuir and Freundlich adsorption isothermal model for the retention of 2,4,5-T.

Langmuir isotherm				Freundlich isotherm		
m_{CLDH} (mg)	Q_m (mg/g)	K (L/mg)	R2	K_F (mg/g)	n	R2
30	590.00	0.009	0.268	1.54	0.75	0.962
50	333.30	0.008	0.375	1.53	0.99	0.959

From the results of Table 5, we can say that the two isotherms obtained agree with the Freundlich model; on the other hand, the Langmuir models give values that prove that it is not valid. However, K_F and n are characteristic parameters of the adsorbate-adsorbent system; the Freundlich constant K_F is related to the adsorption capacity and represents the amount of the pollutant adsorbed on the adsorbent. It can be seen that this constant increases as the retention capacity increases. It can be seen that the K_F constant (Freundlich's constant) increases as the retention capacity increases. The value of the heterogeneity factor 1/n is greater than 1 (n <1); this result probably implies the existence of a more heterogeneous adsorption surface (heterogeneous adsorption sites) [30]. Therefore, the binding of 2,4,5-T anions can be explained by electrostatic interactions, on the one hand, between 2,4,5-T molecules and, on the other hand, by hydrogen bonds between reconstructed LDH sheets and 2,4,5-T anions. If n <1, adsorption is normal and occurs in more than one layer [46]. Thus, we assume that 2,4,5-T molecules are probably double-layered on the surface of reconstructed LDH through π-π interactions of the aromatic ring [47].

2.5. Effect of 2,4,5-T/CLDH mass ratio.

To examine the effect of the adsorbate/adsorbent mass ratio on the adsorption capacity of CLDH, the initial adsorbate concentration was varied from 10 to 500 mg/L while keeping the mass of CLDH constant equal to 30 mg (Fig. 9).

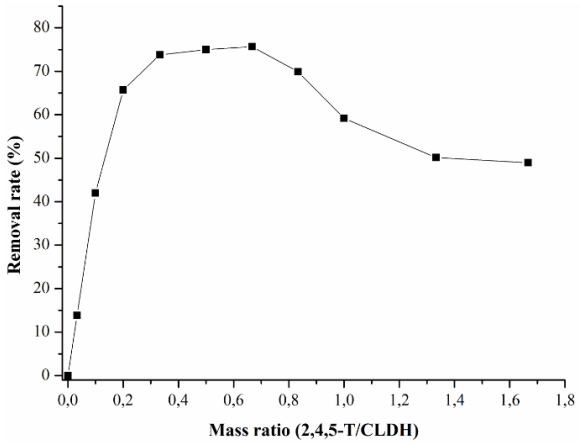

Figure 9. Retention rate of 2,4,5-T as a function of the $m_{2,4,5\text{-}T}/m_{CLDH}$ mass ratio.

It can be deduced that the maximum elimination rate is equal to 75%; it is obtained for an optimum mass ratio of 0.66.

3. Results and Discussion

3.1. XRD study.

The solid compound obtained under optimal conditions after contact with the solution of 2,4,5-T was analyzed by XRD. The spectrum of this phase is shown in Fig. 10c. This

technique provides information on the sheet and the interlayer space. The X-ray diffractogram of the [Zn_2-Al-CO_3] phase obtained by synthesis under optimal conditions (Fig. 10a) is comparable to that of natural hydrotalcite [48]; it shows good crystalline organization. The majority of lines are fine, symmetrical, and intense. All the observed diffraction lines are indexed in a hexagonal cell of rhombohedral symmetry with a space group $R\bar{3}$m. In the calcined LDH phase (Fig. 10b), we see the presence of broad ZnO lines, indicating that the destruction of the sheets leads to the formation of an amorphous phase of the mixed oxides. The intercalation of 2,4,5-T anions between the LDH sheets leads to a shift of the (003) line towards the low 2θ values, which corresponds to an increase in the distance between the sheets to reach 1.05 nm (0.764 nm for [Zn_2-Al-CO_3]).

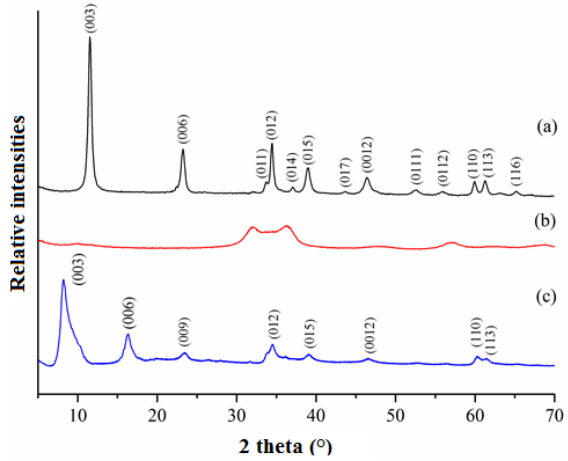

Figure 10. X diffractograms of the LDH matrix (a), calcined LDH (b), and of the phase [Zn_2-Al-2,4,5-T] obtained after retention of 2,4,5-T (c).

3.2. Spectroscopy analysis IR.

The IR spectrum of the phase intercalated by the carbonate anions (Fig. 11a) presents bands around 3470 and 1630 cm^{-1} corresponding respectively to the valence vibrations of the hydroxyl groups of the brucite layers (ν_{OH}) and the deformation vibrations of the molecules water inter-foliar (δ_{H2O}). Also, we observe the band of the metal oxides (O-M-O) around 540 cm^{-1} [49].

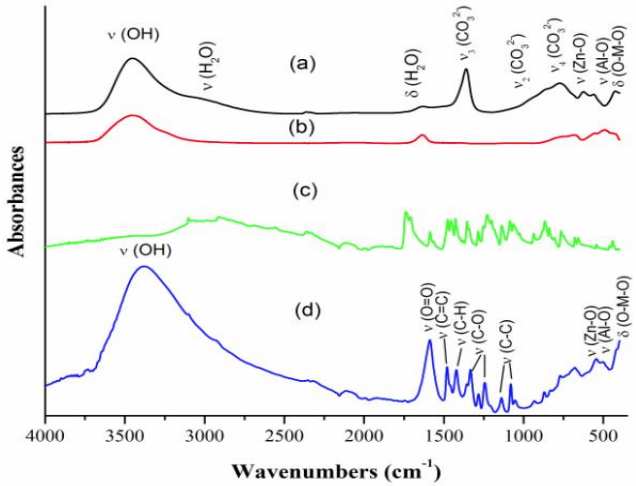

Figure 11. IR spectra of LDH (a), calcined LDH (b), herbicide 2,4,5-T (c) and [Zn_2-Al-2,4,5-T] phases obtained after retention (d).

The IR spectrum of CLDH (Fig. 11b) gives the characteristic vibration bands of OH groups at 3453 cm^{-1}, the Al-O bands at 434 and 532 cm^{-1}, and the Zn-O band around 684 cm^{-1}. The bands corresponding to the vibrations of the carbonate anions have completely disappeared due to their total decomposition [50]. Compared to Fig. 11a, we report the disappearance of the characteristic band of the layers around 400 cm^{-1}, which confirms that the crystalline structure is destroyed after calcination of LDH at 500 °C, in agreement with the XRD results (Fig. 10b).

From the results obtained after retention of 2,4,5-T by CLDH (Fig. 11d), we can notice on the corresponding IR spectrum that the band at 3420 cm^{-1} corresponds to the valence vibrations of OH. The band around 1600 cm^{-1} is characteristic of the vibrations of the carboxylate ions (C=O). The two bands at 1490 cm^{-1} and 1420 cm^{-1} relate to the vibrations (C=C) of the aromatic nucleus. The other two bands, around 1240 cm^{-1} and 1080 cm^{-1}, correspond to the antisymmetric and symmetrical vibrations of (C-O-C). At 860 cm^{-1}, we denote the vibration band of (C-Cl). The band around 780 cm^{-1} is attributed to the vibrations (C-H) of deformation out of the plane. The characteristic bands of the matrix sheets correspond to the metal-oxygen vibrations for (Zn-O), around 542 $cm^{-1,}$ and for (Al-O), around 494 cm^{-1} [51].

3.3. Scanning Electron Microscopy (SEM) analysis.

The SEM image corresponding to the calcined LDH phase is shown in Fig. 12a. the lamellar character is absent due to the destruction of the LDH sheets and the appearance of aggregates corresponding to the mixed oxides. The phase obtained after retention of 2,4,5-T (Fig. 12b) is in the form of aggregates consisting of crystallites of different sizes. This result confirms that after retention of 2,4,5-T by CLDH, we see the appearance of the lamellar character using the memory effect retained by the mixed oxides obtained by the calcination of the initial LDH [52].

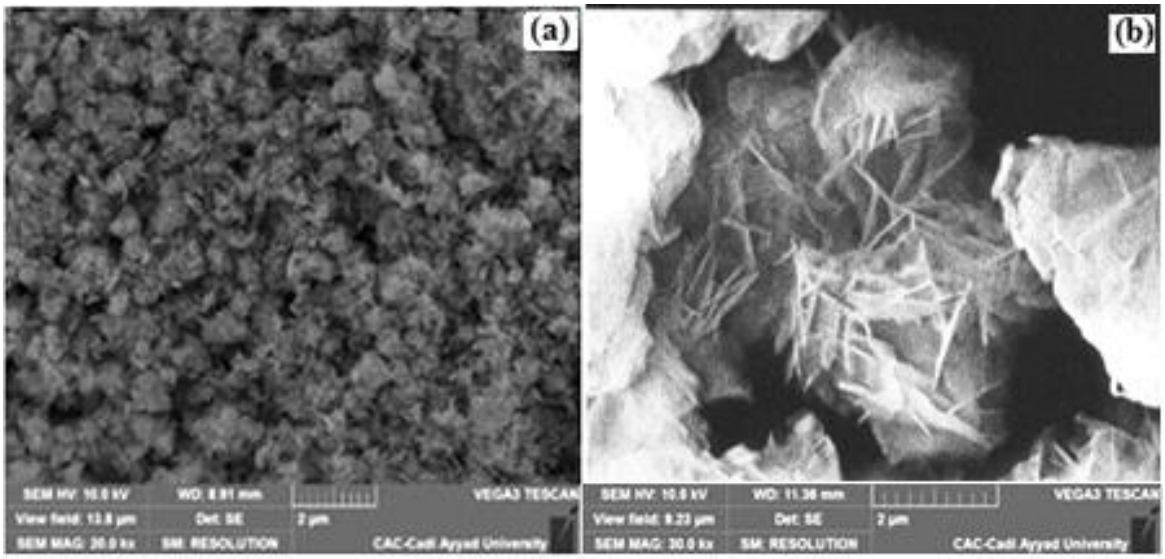

Figure 12. SEM images of the calcined phase (a) and of the phase [Zn_2-Al-2,4,5-T] (b) obtained after retention.

The X-ray emission microanalysis spectrum of the compound [Zn_2-Al-2,4,5-T] (Fig. 13) shows, in addition to emissions of zinc and aluminum, emissions of chlorine, carbon, and oxygen, confirming the intercalation of 2,4,5-T.

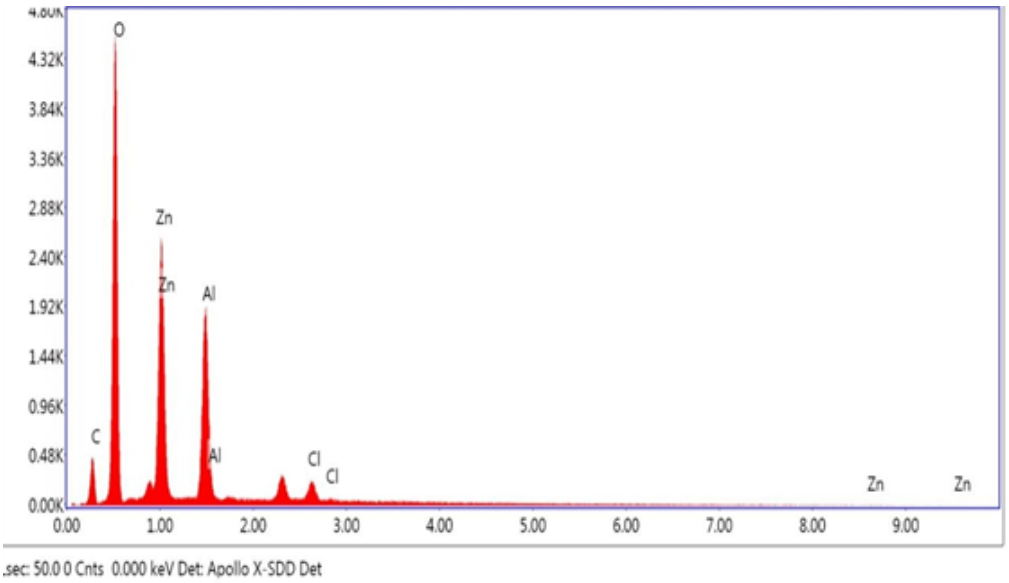

Figure 13. X-ray emission spectrum of phase [Zn_2-Al-2,4,5-T] obtained after retention of 2,4,5-T.

3.4. Structural model.

In Figure 14, we have proposed the most probable orientation of the 2,4,5-T pollutant interposed between the LDH sheets.

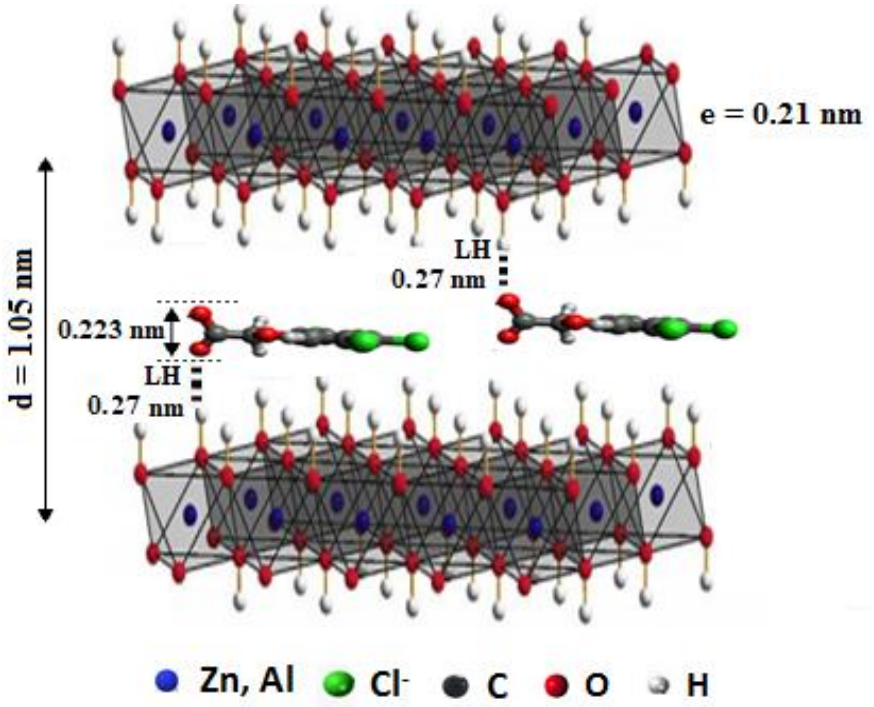

Figure 14. Structural orientation model of 2,4,5-T between LDH sheets.

The interlamellar distance, determined experimentally equal to 1.05 nm, requires that the carboxylate groups (COO^-) be oriented towards the LDH sheets, suggesting a horizontal arrangement of the 2,4,5-T anion. This arrangement leads to an interlamellar dimension of 2,4,5-T of 0.223 nm. Knowing the thickness of the LDH sheet, which is equal to 0.21 nm, and the length of the hydrogen bond, which is of the order of 0.27 nm, we will have:

$$d = 0.27 + 0.27 + 0.21 + 0.223 = 0.973 \text{ nm} < 1.05 \text{ nm}$$

It can be seen that the theoretically determined distance is less than that found experimentally, which can probably be explained by the existence of a single hydrogen bond between each 2,4,5-T anion and one of the reconstructed LDH sheets.

3.5. Recycling and regeneration of CLDH material.

The efficiency of 2,4,5-T removal by CLDH depends on the percentage of 2,4,5-T remaining after a series of regeneration cycles while working with a mass ratio $m_{2,4,5\text{-}T}/m_{CLDH}$ of 0.66, which corresponds to a maximum retention of 75% of 2,4,5-T. To replace the 2,4,5-T ions retained after reconstruction, an exchange with a 1M Na_2CO_3 solution is carried out because the carbonates have a very high affinity for the LHD adsorbent [53]. In Fig. 15, we see the percentage of 2,4,5-T retained from the different solutions after a series of retention, exchange, and calcination.

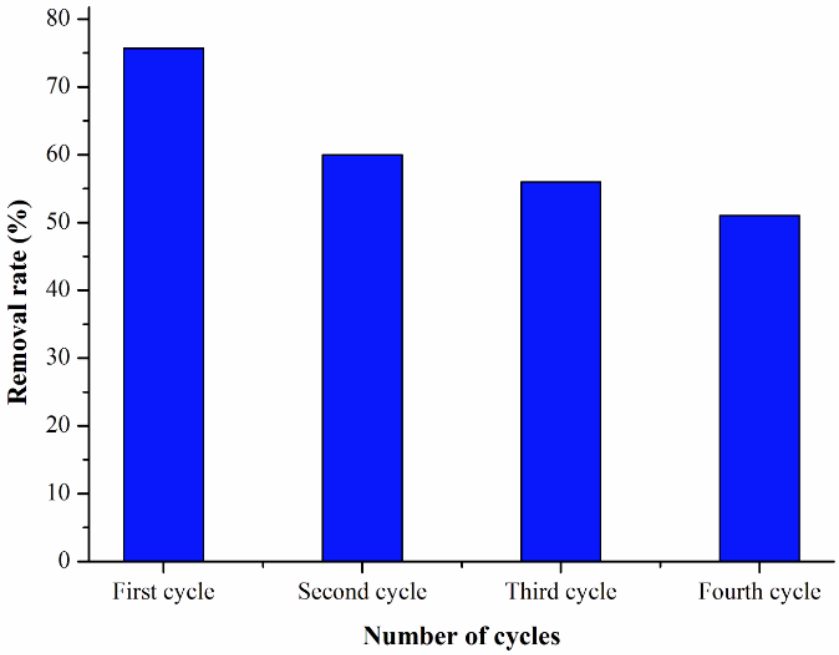

Figure 15. Regeneration and recycling efficiency of LDH after retention 2,4,5-T for a mass ratio of 0.66.

The 2,4,5-T removal rate decreases from 75% to 49 % after four recycling cycles. This indicates that the material used can be considered a potential adsorbent for the retention of 2,4,5-T and that it is moderately recyclable in the case of this pollutant.

3.6. Comparative studies.

In this study, we present the results of several researchers who have worked on retaining 2,4,5-T pesticides with different adsorbent materials. We will compare their retention capacities and removal rates, which are two indicators to demonstrate pollutants' effectiveness and elimination capacity. The summary of the results is quoted in Table 6.

Table 6. Maximum adsorption capacities and removal rates of 2,4,5-T pesticide on different materials.

Adsorbents	Q_m (mg/g)	Removal rate (%)	References
Zn_2-Al-Cl	718	96	[22]
Activated Carbon	178.57	-	[54]
$Al(OH)_3$	43.25	86	[55]
MgFe-LDH	13	50	[56]
Calcined Zn_2-Al-CO_3	590	75	*This work*

The calcined adsorbent Zn_2-Al-CO_3 used in this study has been shown to be very efficient and eco-friendly because it does not generate sludge in an aquatic environment. Comparing the used adsorbent material with other adsorbents shows it is competitive and promising for eliminating anionic pesticides from wastewater.

4. Conclusions

Calcined LDH material has shown its adsorption efficiency against the pollutant 2,4,5-T in an aqueous solution. The results show that the adsorption capacity increases with a decrease in the mass of CLDH regardless of the initial concentration of 2,4,5-T in the solution. This confirms that the cost can be minimized by using small amounts of the carrier with the elimination of 2,4,5-T. Kinetic adsorption modeling shows that the pseudo-second-order model best describes adsorption kinetics, with an equilibrium contact time of 6h. The study of adsorption isotherms shows that the Freundlich model correctly describes the adsorption process with correlation coefficient values close to unity. The maximum retention (75%) of 2,4,5-T is obtained for an optimal 2,4,5-T/CLDH mass ratio of 0.66 with an experimental retention capacity that exceeds 590 mg/g. The results of the four complementary techniques used (XRD, IR, and SEM-EDX) confirm the retention of 2,4,5-T by surface adsorption and intercalation between the reconstructed LDH sheets. The calcined material used has demonstrated its effectiveness with a relatively better capacity than other adsorbents for removing this potential pollutant and with the possibility of its recycling.

Funding

This research received no external funding.

Acknowledgments

The authors thank the Department of Chemistry, Teacher's Training School, Cadi Ayyad University of Marrakesh.

Conflicts of Interest

The authors declare no conflict of interest.

References

1. Li, X.; Liu, C.; Liu, F.; Zhang, X.; Peng, Q.; Wu, G.; Zhao, Z. Accelerated removal of five pesticide residues in three vegetables with ozone microbubbles. *Food Chem.* **2023**, *403*, https://doi.org/10.1016/j.foodchem.2022.134386.
2. Wang, L.B.; Wang, J.J.; Yue, E.L.; Li, J.F.; Tang, L.; Bai, C.; Chen, X.L. Water-Stable Cd-MOF with fluorescent sensing of Tetracycline, Pyrimethanil, abamectin benzoate and construction of logic gate. *Spectrochim. Acta A Mol. Biomol. Spectrosc*. **2023**, *285*, https://doi.org/10.1016/j.saa.2022.121894.
3. Li, H.X.; Han, S.B.; Wu, X.; Wang, S.; Liu, W.P.; Ma, T.; Wei, S.B. Distribution, characteristics and influencing factors of fresh groundwater resources in the Loess Plateau. *China. Geol. China* **2021**, *4*, 509-526, https://doi.org/10.31035/cg2021057.
4. Tiller, R.; Booth, A.; Kubowicz, S.; Jahren, S. Co-production of future scenarios of policy action plans in a science-policy-industry interface–The case of microfibre pollution from wastewater treatment plants in Norway. *Mar. Pollut. Bull.* **2021**, *173*, https://doi.org/10.1016/j.marpolbul.2021.113062.
5. Campanale, C.; Massarelli, C.; Losacco, D.; Bisaccia, D.; Triozzi, M.; Uricchio, V.F. The monitoring of pesticides in water matrices and the analytical criticalities: A review. *TrAC, Trends Anal. Chem.* **2021**, *144*, https://doi.org/10.1016/j.trac.2021.116423.

6. Khan, N.A.; Khan, S.U.; Ahmed, S.; Farooqi, I.H.; Yousefi, M.; Mohammadi, A.A.; Changani, F. Recent trends in disposal and treatment technologies of emerging-pollutants-A critical review. *Trends Anal. Chem.* **2020a**, *122*, https://doi.org/10.1016/j.trac.2019.115744.
7. Khan, N.A.; Ahmed, S.; Farooqi, I.H.; Ali, I.; Vambol, V.; Changani, F.; Khan, A.H. Occurrence, sources and conventional treatment techniques for various antibiotics present in hospital wastewaters: a critical review. *Trends Anal. Chem.* **2020b**, *129*, https://doi.org/10.1016/j.trac.2020.115921.
8. Akdemir Evrendilek, G.; Keskin, E.; Golge, O. Interaction and multi-objective effects of multiple non-thermal treatments of sour cherry juice: pesticide removal, microbial inactivation, and quality preservation. *J. Sci. Food Agric.* **2020**, *100*, 1653-1661, https://doi.org/10.1002/jsfa.10178.
9. Rodrigues, T.F.; Bender, F.R.; Sanzovo, A.W.S.; Ferreira, E.; Nogueira, M.A.; Hungria, M. Impact of pesticides in properties of Bradyrhizobium spp. and in the symbiotic performance with soybean. *World J. Microbiol. Biotechnol.* **2020**, *36*, 1-16, https://doi.org/10.1007/s11274-020-02949-5.
10. Mir, S.A.; Dar, B.N.; Mir, M.M.; Sofi, S.A.; Shah, M.A.; Sidiq, T.; Sunooj, K.V.; Hamdani, A.M.; Khaneghah, A.M. Current strategies for the reduction of pesticide residues in food products. *J. Food Compos. Anal.* **2022**, *106*, https://doi.org/10.1016/j.jfca.2021.104274.
11. Nowell, L.H.; Moran, P.W.; Bexfield, L.M.; Mahler, B.J.; Van Metre, P.C.; Bradley, P.M.; Qi, S.L. Is there an urban pesticide signature? Urban streams in five US regions share common dissolved-phase pesticides but differ in predicted aquatic toxicity. *Sci. Total Environ.* **2021**, *793*, https://doi.org/10.1016/j.scitotenv.2021.148453.
12. Janney, P.; Jenkins, J. Passive sampling and ecohydrologic modeling to investigate pesticide surface water loading in the Zollner Creek watershed, Oregon, USA. *Sci. Total Environ.* **2022**, *819*, https://doi.org/10.1016/j.scitotenv.2022.152955.
13. Jatoi, A.S.; Hashmi, Z.; Adriyani, R.; Yuniarto, A.; Mazari, S.A.; Akhter, F.; Mubarak, N.M. Recent trends and future challenges of pesticide removal techniques–a comprehensive review. *J. Environ. Chem. Eng.* **2021**, *9*, https://doi.org/10.1016/j.jece.2021.105571.
14. Wilson, C.; Tisdell, C. Why farmers continue to use pesticides despite environmental, health and sustainability costs. *Ecol. Econ.* **2001**, *39*, 449-462, https://doi.org/10.1016/S0921-8009(01)00238-5.
15. Moinina, A.; Lahlali, R.; MacLean, D.; Boulif, M. Farmers' Knowledge, Perception and Practices in Apple Pest Management and Climate Change in the Fes-Meknes Region, Morocco. *Horticulturae* **2018**, *4*, https://doi.org/10.3390/horticulturae4040042.
16. Gupta, P.; Pandey, K.; Verma, N. Augmented complete mineralization of glyphosate in wastewater via microbial degradation post CWAO over supported Fe-CNF. *J. Chem. Eng.* **2022**, *428*, https://doi.org/10.1016/j.cej.2021.132008.
17. Chhokar, R.S.; Singh, S.; Sharma, R.K. Herbicides for control of isoproturon-resistant Littleseed Canarygrass (Phalaris minor) in wheat. *J. Crop Prot.* **2008**, *27*, 719-726, https://doi.org/10.1016/j.cropro.2007.10.004.
18. Wang, D.; Mukome, F.N.; Yan, D.; Wang, H.; Scow, K.M.; Parikh, S.J. Phenylurea herbicide sorption to biochars and agricultural soil. *J. Environ. Sci. Health B* **2015**, *50*, 544-551, https://doi.org/10.1080/03601234.2015.1028830.
19. Giacomazzi, S.; Cochet, N. Environmental impact of diuron transformation: a review. *Chemosphere* **2004**, *56*, 1021-1032, https://doi.org/10.1016/j.chemosphere.2004.04.061.
20. Ugbede Itodo, H. Controlled release of herbicides using nano-formulation: a review. *Chem. Rev.* **2019**, *1*, 130-138, https://doi.org/10.33945/SAMI/JCR.2019.2.4.
21. Pandiarajan, A.; Kamaraj, R.; Vasudevan, S.; Vasudevan, S. OPAC (orange peel activated carbon) derived from waste orange peel for the adsorption of chlorophenoxyacetic acid herbicides from water: adsorption isotherm, kinetic modelling and thermodynamic studies. *Bioresour. Technol.* **2018**, *261*, 329-341, https://doi.org/10.1016/j.biortech.2018.04.005.
22. Mourid, E.H.; Lakraimi, M.; Legrouri, A. Removal and Release of the 2, 4, 5-Trichlorophenoxyacetic Acid Herbicide from Wastewater by Layered Double Hydroxides. *J. Inorg. Organomet. Polym. Mater.* **2021**, *31*, 2116-2128, https://doi.org/10.1007/s10904-020-01845-7.
23. Rana, A.K.; Mishra, Y.K.; Gupta, V.K.; Thakur, V.K. Sustainable materials in the removal of pesticides from contaminated water: perspective on macro to nanoscale cellulose. *Sci. Total Environ.* **2021**, *797*, https://doi.org/10.1016/j.scitotenv.2021.149129.
24. Obayomi, K.S.; Lau, S.Y.; Danquah, M.; Chiong, T.; Takeo, M. Advances in graphene oxide based nanobiocatalytic technology for wastewater treatment. *Environ. Nanotechnol. Monit. Manag.* **2022**, *17*, https://doi.org/10.1016/j.enmm.2022.100647.
25. Zieliński, B.; Miądlicki, P.; Przepiórski, J. Development of activated carbon for removal of pesticides from water: case study. *Sci. Rep.* **2022**, *12*, 1-14, https://doi.org/10.1038/s41598-022-25247-6.
26. Hagner, M.; Mikola, J.; Saloniemi, I.; Saikkonen, K.; Helander, M. Effects of a glyphosate-based herbicide on soil animal trophic groups and associated ecosystem functioning in a northern agricultural field. *Sci. Rep.* **2019**, *9*, 1-13, https://doi.org/10.1038/s41598-019-44988-5.
27. Hassaan, M.A.; El Nemr, A. Pesticides Pollution: Classifications, Human Health Impact, Extraction and Treatment Techniques. *Egypt. J. Aquat. Res.* **2020**, *46*, 207-220, https://doi.org/10.1016/j.ejar.2020.08.007.

28. Ansari, I.; El-Kady, M.M.; Arora, C.; Sundararajan, M.; Maiti, D.; Khan, A. 16 - A review on the fatal impact of pesticide toxicity on environment and human health. *Glob. Climate. Change* **2021**, 361-391, https://doi.org/10.1016/B978-0-12-822928-6.00017-4.
29. Rosic, N.; Bradbury, J.; Lee, M.; Baltrotsky, K.; Grace, S. Corrigendum to "The impact of pesticides on local waterways: A scoping review and method for identifying pesticides in local usage. *Environ. Sci. Policy* **2021**, *128*, https://doi.org/10.1016/j.envsci.2021.11.005.
30. Zeng, F.; Cao, S.; Jin, W.; Zhou, X.; Ding, W.; Tu, R.; Ding, F. Inactivation of chlorine-resistant bacterial spores in drinking water using UV irradiation, UV/Hydrogen peroxide and UV/Peroxymonosulfate: Efficiency and mechanism. *J. Clean. Prod.* **2020**, *243*, https://doi.org/10.1016/j.jclepro.2019.118666.
31. Kotp, Y.H. Enhancement of industrial effluents quality by using nanocomposite Mg/Al LDH ultrafiltration membranes. *J. Inorg. Organomet. Polym. Mater.* **2020**, *30*, 5244-5260, https://doi.org/10.1007/s10904-020-01608-4.
32. Zazou, H.; Oturan, N.; Zhang, H.; Hamdani, M.; Oturan, M.A. Comparative study of electrochemical oxidation of herbicide 2,4,5-T: kinetics, parametric optimization and mineralization pathway. *Sustain. Environ. Res.* **2016**, *27*, 15–23, https://doi.org/10.1016/j.serj.2016.11.008.
33. Andreotti, G.; Beane Freeman, L.E.; Shearer, J.J.; Lerro, C.C.; Koutros, S.; Parks, C.G.; Hofmann, J.N. Occupational pesticide use and risk of renal cell carcinoma in the agricultural health study. *Environ. Health Perspect.* **2020**, *128*, https://doi.org/10.1289/EHP6334.
34. Prytula, M.T.; Pavlostathis, S.G. Effect of contaminant and organic matter bioavailability on the microbial dehalogenation of sediment-bound chlorobenzenes. *Water Res.* **1996**, *30*, 2669-2680, https://doi.org/10.1016/S0043-1354(96)00180-7.
35. Hoshino, K.; Furuya, S.; Buchheit, R.G. Effect of Solution pH on Layered Double Hydroxide Formation on Electrogalvanized Steel Sheets. *J. Mater. Eng. Perform.* **2019**, *28*, 2237–2244, https://doi.org/10.1007/s11665-019-03963-x.
36. Catherine, H.N.; Ou, M.H; Manu, B.; Shih, Y.H. Adsorption mechanism of emerging and conventional phenolic compounds on graphene oxide nanoflakes in water. *Sci. Total Environ.* **2018**, *635*, 629-638, https://doi.org/10.1016/j.scitotenv.2018.03.389.
37. Emmanuel Revellame, D.; Fortela, D.L.; Sharp, W.; Hernandez, R.; Mark Zappi, E. Adsorption kinetic modeling using pseudo-first order and pseudo-second order rate laws: A review, *Clean. Eng. Technol.* **2020**, *1*, https://doi.org/10.1016/j.clet.2020.100032.
38. Moussout, H.; Ahlafi, H.; Aazza, M.; Maghat, H. Critical of linear and nonlinear equations of pseudo-first order and pseudo-second order kinetic models. *Karbala Int. J. Mod. Sci.* **2018**, *4*, 244-254, https://doi.org/10.1016/j.kijoms.2018.04.001.
39. Russo, V.; Rossano, C.; Salucci, E.; Tesser, R.; Salmi, T.; Di Serio, M. Intraparticle diffusion model to determine the intrinsic kinetics of ethyl levulinate synthesis promoted by Amberlyst-15. *Chem. Eng. Sci.* **2020**, *228*, https://doi.org/10.1016/j.ces.2020.115974.
40. Crini, G.; Badot, P.M. Application of chitosan, a natural aminopolysaccharide, for dye removal from aqueous solutions by adsorption processes using batch studies: A review of recent literature. *Prog. Polym. Sci.* **2008**, *33*, 399-447, https://doi.org/10.1016/j.progpolymsci.2007.11.001.
41. Ebelegi, A.; Ayawei, N.; Wankasi, D. Interpretation of Adsorption Thermodynamics and Kinetics. *Open J. Phys. Chem.* **2020**, *10*, 166-182, https://doi.org/10.4236/ojpc.2020.103010.
42. Mustapha, S.; Shuaib, D.T.; Ndamitso, M.M.; Etsuyankpa, M.B.; Sumaila, A.; Mohammed, U.M.; Nasirudeen, M.B. Adsorption isotherm, kinetic and thermodynamic studies for the removal of Pb(II), Cd(II), Zn(II) and Cu(II) ions from aqueous solutions using Albizia lebbeck pods. *Appl. Water. Sci.* **2019**, *9*, https://doi.org/10.1007/s13201-019-1021-x.
43. Al-Ghouti, M.A.; Da'ana, D.A. Guidelines for the use and interpretation of adsorption isotherm models: A review. *J. Hazard. Mater.* **2020**, *393*, https://doi.org/10.1016/j.jhazmat.2020.122383.
44. Langmuir, I. The adsorption of gases on plane surfaces of glass, mica and platinum. *J. Am. Chem. Soc.* **1918**, *40*, 1361-1403, https://doi.org/10.1021/ja02242a004.
45. Freundlich, H.M.F. Over the Adsorption in Solution. *J. Phys. Chem.* **1906**, *57*, 385-471.
46. Kamga, F.T. Modeling adsorption mechanism of paraquat onto Ayous (Triplochiton scleroxylon) wood sawdust. *Appl. Water Sci.* **2019**, *9*, 1-7, https://doi.org/10.1007/s13201-018-0879-3.
47. Berber, M.R. Current advances of polymer composites for water treatment and desalination. *J. chem.* **2020**, *2020*, https://doi.org/10.1155/2020/7608423.
48. Bai, S.; Chu, H.; Xiang, X.; Luo, R.; He, J.; Chen, A. Fabricating of Fe_2O_3/$BiVO_4$ heterojunction based photoanode modified with NiFe-LDH nanosheets for efficient solar water splitting. *J. Chem. Eng.* **2018**, *350*, 148-156, https://doi.org/10.1016/j.cej.2018.05.109.
49. Abniki, M.; Moghimi, A.; Azizinejad, F. Fabrication of bionanocomposite based on LDH using biopolymer of gum arabic and chitosan-coating for sustained drug-release. *J. Serbian Chem. Soc.* **2020**, *85*, 1223-1235, https://doi.org/10.2298/JSC191011004A.
50. Abderrazek, K.; Uheida, A.; Seffen, M.; Muhammed, M.; Frini Srasra, N.; Srasra, E. Photocatalytic degradation of indigo carmine using [Zn-Al] LDH supported on PAN nanofibres. *Clay Miner.* **2015**, *50*, 185-197, https://doi.org/10.1180/claymin.2015.050.2.03.

51. Hoggas, K.; Nouveau, C.; Djelloul, A.; Bououdina, M. Structural, microstructural, and optical properties of $Zn_{1-x}Mg_xO$ thin films grown onto glass substrate by ultrasonic spray pyrolysis. *Appl. Phys. A.* **2015**, *120*, 745-755, https://doi.org/10.1007/s00339-015-9252-7.
52. Santos, R.M.M.; Tronto, J.; Briois, V.; Santilli, C.V. Thermal decomposition and recovery properties of ZnAl–C_{O3} layered double hydroxide for anionic dye adsorption: insight into the aggregative nucleation and growth mechanism of the LDH memory effect. *J. Mater. Chem. A.* **2017**, *5*, 9998-10009, https://doi.org/10.1039/C7TA00834A.
53. Hashim, N.; Sharif, S.N.M.; Muda, Z.; Isa, I.M.; Bakar, S.A.; Ali, N.M.; Hussein, M.Z.; Mamat, M. Release behavior of dichlorprop from Zn/Al-ldh-dichlorprop nanocomposite into chloride, carbonate and phosphate solutions. *J. Teknol.* **2019**, *81*, 1-10, https://doi.org/10.11113/jt.v81.12919.
54. Hue, H.K.; Anh, L.V.; Trong, D.B. Study of the adsorption of 2,4-dichlorophenoxyacetic acid from the aqueous solution onto activated carbon. *Vietnam J. Chem.* **2018**, *56*, 208-213, https://doi.org/10.1002/vjch.201800015.
55. Kamaraj, R.; Vasudevan, S. Facile one-pot electrosynthesis of Al $(OH)_3$–kinetics and equilibrium modeling for adsorption of 2, 4, 5-trichlorophenoxyacetic acid from aqueous solution. *New J. Chem.* **2016**, *40*, 2249-2258, https://doi.org/10.1039/C5NJ02407B.
56. Phuong, N.T.K.; Beak, M.W.; Huy, B.T.; Lee, Y.I. Adsorption and photodegradation kinetics of herbicide 2, 4, 5-trichlorophenoxyacetic acid with MgFeTi layered double hydroxides. *Chemosphere* **2016**, *146*, 51-59, https://doi.org/10.1016/j.chemosphere.2015.12.008.